PERGAMON

International Journal of Multiphase Flow 27 (2001) 861–883

International Journal of Multiphase Flow

www.elsevier.com/locate/ijmulflow

Droplet size measurements in horizontal annular gas–liquid flow

Mark J.H. Simmons *, Thomas J. Hanratty

Department of Chemical Engineering, University of Illinois, Urbana, IL 61801, USA

Received 4 February 2000; received in revised form 8 September 2000

Abstract

Measurements of drop size distributions in air–water annular flow have been made in a horizontal 0.0953 m pipe, at atmospheric pressure. A laser diffraction technique has been employed, using a Malvern Spraytec R5008 instrument. Stratification of the droplets has been observed by obtaining measurements at the pipe centre line, and 0.019 m above and below it. The stratification, which is caused by the effects of gravitational settling and the asymmetry of the liquid film, decreases with increasing gas velocity. Measured Sauter mean diameters at the pipe centre are similar to what has been observed in vertical pipes. However, they show a stronger effect of liquid flow rate than predicted by the correlation of Azzopardi, that was developed from measurements made with an earlier diffraction technique that did not account for multiple scattering. A log-normal or an upper limit log-normal distribution underpredicts the measured contributions of small diameter drops. © 2001 Elsevier Science Ltd. All rights reserved.

Keywords: Gas–liquid pipe flow; Annular flow; Drop size distributions; Malvern Spraytec; Laser diffraction; Droplet stratification

1. Introduction

Several different flow patterns can exist for the simultaneous co-current flow of gas and liquid in a conduit. The term annular flow is used to describe a condition for which some of the liquid travels as a film on the wall and some, as droplets in the gas. It is a common pattern in industrial equipment where the quality (vapour mass fraction) is changing, as in a boiler tube. Annular flow can occur at all pipe orientations, and the fraction of liquid carried as droplets can vary from zero

* Corresponding author. Present address: School of Chemical Engineering, University of Birmingham, Edgbaston, Birmingham B15 2TT, UK. Tel.: +121-414-5371; fax: +121-414-5324.

E-mail address: m.j.simmons@bham.ac.uk (M.J.H. Simmons).

PII: S0301-9322(00)00053-7

to a value close to unity. Droplets deposit onto the wall and waves present on the liquid film are entrained in the gas. For a fully developed flow, the fraction of the liquid entrained as drops, E, is described as a balance between the rates of atomisation and deposition. The prediction requires knowledge of the distribution of drop sizes in the gas core. This paper presents measurements of drop sizes for air and water flowing in an annular pattern in a horizontal 0.0953 m pipe, at atmospheric pressure.

A thorough review of drop size measurements in annular flows has been presented by Azzopardi (1997). Several techniques have been employed: Tatterson et al. (1977) used charge removal from an insulated probe. Wicks and Dukler (1966) used a needle bridging method, where two needles were placed a small distance apart and connected to a resistance and a battery. Drops larger than the gap completed the circuit and caused an electrical pulse. By varying the needle gap, the cumulative size distribution was obtained. Semiat and Dukler (1981) and Lopes and Dukler (1985) used a laser grating technique, which produced a local measurement of drop size and velocity. All these techniques were unable to detect very small drops, below 100–200 μm. Subsequent work has shown that these techniques lead to significant error in measuring the volume median size since a significant proportion of the volume is carried by drops smaller than 100 μm. Further refinements were made to the laser-grating technique by Fore and Duker (1995). These allowed measurement of droplets down to a size of 10 μm.

Several workers have used photographic methods (Cousins and Hewitt (1968), Pogson et al. (1970), Andreussi et al., 1978). A problem with these techniques is that they, too, can favour large drops, since it is more probable that part of a large droplet may be within the field of the camera lens. Furthermore, smaller droplets may not be detected since they could be out of focus, particularly if the resolution of the photographs is poor. Hay et al. (1996) addressed this problem by using a sheet of laser light to illuminate the flow field. The laser sheet was thinner than the focal depth of the camera lens, so only droplets illuminated by the laser sheet appeared in focus. Droplets out of focus were eliminated from the analysis by examining changes in the light gradient at the edges of the drops.

A laser diffraction technique, invented by Swithenbank et al. (1976), has been used by several workers. This work has been reviewed by Azzopardi (1997). Instruments based on this approach are marketed by Malvern Instruments. Early versions required the assumption of a distribution function for drop size, either the equation of Rosin and Rammler (1933) or the upper limit log-normal distribution of Mugele and Evans (1951). Current versions employ a 15 parameter "model independent" algorithm which does not impose any unimodal distribution function. The detection range of the instrument is governed by the focal length of the lens used in the detector. Combellack and Matthews (1981) and Azzopardi (1985) indicated the importance of using the optimal focal length.

The use of the diffraction technique has been limited to situations in which the concentration of droplets is low. The algorithms used to analyse the measurements assume that the light is scattered only by one drop. At higher concentrations, multiple scattering of laser light by many drops can exist. This will cause the scattered light to enter the detector at a larger angle; the distributions obtained will overpredict the number of smaller drops. Harvill et al. (1997) developed a patented multiple scattering algorithm to correct for this effect. This is employed in the Malvern Spraytec R5000 series of instruments used in this study.

Because a large number of techniques have been employed in different flow systems, it is difficult to ascertain whether differences in drop size distributions could be caused by artefacts of the system or the technique. One problem, already mentioned, is associated with the range of drop sizes that are detected. Simmons et al. (2000) compared measurements of a 90–106 μm sieve cut of glass beads suspended in water using Malvern 2600, Phase Doppler and Par-Tec instruments. Reasonable agreement was found with an independent measurement obtained by photography. However, it must be noted that the size range of the glass beads was much narrower than would be found in an annular flow.

Most of the available data are for vertical annular flows. Limited amount of data have been obtained for horizontal annular flows and incomplete observations of the effects of horizontal stratification and of the pipe diameter remain a concern. Wicks and Dukler (1966) presented some data, but the analysis of the measurements was shown to be flawed by McVean and Wallis (1969). Zaidi et al. (1998) compared drop size measurements for air–water annular flow in a 0.038-m pipe obtained with Phase Doppler and Malvern 2600 systems for a range of inclinations from horizontal to vertical downward and discovered noticeable differences in the size distributions. Azzopardi et al. (1996) used a Malvern 2600 particle sizer mounted horizontally on a 0.063-m pipe and found significant horizontal stratification of the droplet sizes. The study was limited to superficial gas velocities of 25 m/s, where an atomising stratified flow exists. Ribeiro et al. (1995) obtained drop sizes for air–water flow at higher gas velocities in a horizontal 0.032-m pipe with a similar instrument. However, observation of horizontal stratification of the drops was not possible because the unit was mounted vertically.

This paper presents new measurements of drop size distributions, made at three vertical positions in a horizontal pipe, with a Malvern Spraytec R5008 particle sizer. Use of a multiple-scattering algorithm has allowed valid measurements to be made in a larger diameter pipe and at higher liquid concentrations than investigated previously. Studies were made at gas superficial velocities of 30–50 m/s and liquid superficial velocities of 0.016–0.12 m/s. Stratification of the droplets was observed. The drop size measurements are compared with different droplet distribution functions.

2. Theory

2.1. Drop distribution functions

A representation of the drop sizes found in annular flows can be made by assuming a distribution function. The large number of fine particles has made it difficult to measure the total number of particles. Therefore, a normalised volume distribution function, f_v has been used. This is defined as

$$\frac{dv}{dd_p} = f_v(d_p), \tag{1}$$

$$\int_0^\infty f_v(d_p)\,dd_p = 1 \tag{2}$$

and

$$f_n(d_p)d_p^3 \mathrm{d}d_p = f_v(d_p)\mathrm{d}d_p, \tag{3}$$

where d_p is the particle diameter and f_n is a normalised number distribution function. Since the volume of a particle is proportional to d_p^3, the volume distribution is more highly skewed in the direction of large d_p than is the number distribution. Further details are given by Tatterson et al. (1977).

The upper limit log-normal (ULLN) distribution, developed by Mugele and Evans (1951), to describe drop size distributions in atomising jets, has been used for annular flows by Tatterson et al. (1977), Lopes and Dukler (1985), Andreussi et al. (1978) and Hay et al. (1996). It can be written in the form

$$f_v(d_p) = \frac{\delta d_{max}}{\sqrt{\pi} d_p (d_{max} - d_p)} \exp(-\delta^2 z^2), \tag{4}$$

where

$$z = \ln\left[\frac{a d_p}{d_{max} - d_p}\right], \tag{5}$$

$$a = \frac{d_{max} - d_{v50}}{d_{v50}}. \tag{6}$$

Here, d_{v50} is the volume median diameter and δ is the deviation about the mean. The distribution function is characterised by the parameters d_{max}, d_{v50} and δ.

The function of Rosin and Rammler (1933) has been applied to annular flows by Azzopardi et al. (1978, 1991, 1983), Jepson et al. (1989, 1990), Gibbons (1985), Teixeira et al. (1988), Hay et al. (1996) and Jepson (1992). It is usually given as a cumulative volume distribution

$$F_v(d_p) = 1 - \exp\left[\left(-\frac{d_p}{\overline{X}}\right)^N\right], \tag{7}$$

where N and $\overline{X}$ are empirical constants.

Mean drop sizes are usually defined with a Sauter mean diameter (Crowe et al., 1998). It is more appropriate than a number mean since it represents the drop size that contains most of the volume

$$d_{32} = \frac{\int_0^{d_{max}} d^3 f_n(d_p)\mathrm{d}d_p}{\int_0^{d_{max}} d^2 f_n(d_p)\mathrm{d}d_p}. \tag{8}$$

Substituting from (3) into this expression gives

$$d_{32} = \frac{\int_0^{d_{max}} f_v(d_p)\mathrm{d}d_p}{\int_0^{\mathrm{d}_{max}} d_p^{-1} f_v(d_p)\mathrm{d}d_p}. \tag{9}$$

2.2. Prediction of d_{32}

Experiments in vertical flow have shown that d_{32} varies roughly as U_G^{-1}, where U_G is the actual gas phase velocity, so Tatterson et al. (1977) suggested that

$$\left(\frac{\rho_G U_G^2 d_p}{\sigma}\right)^{0.5}\left(\frac{d_p}{\lambda}\right)^{0.5} = \text{constant}, \tag{10}$$

where λ is the wavelength of the waves on the liquid film which break up to produce droplets. They assumed that λ varies directly with film thickness, m, and argued that m is proportional to the pipe diameter. Azzopardi (1985) developed the following empirical relationship from a consideration of experimental data, which showed $d_{32} \sim U_G^{-1.16}$, and an effect of the liquid flow rate

$$d_{32} = \lambda_A \left[15.4\left(\frac{\rho_L U_G^2 \lambda_A}{\sigma}\right)^{-0.58} + 3.5\left(\frac{G_{LE}}{\rho_L U_G}\right)\right], \tag{11}$$

where G_{LE} is the entrained liquid mass flux. Pan and Hanratty (2000) used a modified form of the above equation. They argued that it is difficult to reconcile the use of ρ_L in the first term inside the brackets with proposed mechanisms of atomisation, that would be expected to be influenced by the kinetic energy of the gas.

$$d_{32} = \lambda_A \left[A\left(\frac{\rho_G U_G^2 \lambda_A}{\sigma}\right)^{-0.58} + B\left(\frac{G_{LE}}{\rho_L U_G}\right)\right], \tag{12}$$

where λ_A is a Taylor length scale defined by Azzopardi

$$\lambda_A = \left(\frac{\sigma}{\rho_L g}\right)^{0.5}. \tag{13}$$

The constants in (12), A and B, were evaluated from (11) by Pan and Hanratty (2000) as 0.33 and 3.5, respectively. An earlier form of (11), proposed by Azzopardi et al. (1980), used the pipe diameter as an alternative length scale. Gibbons (1985) measured drop sizes in a 0.125-m vertical pipe and found only small differences from the data obtained by Azzopardi (1985). Therefore, he suggested that pipe diameter should be abandoned as a length scale.

Ambrosini and Andreussi (1991) modified the correlation developed by Tatterson et al. (1977) with m substituted for wavelength, λ

$$\frac{d_{32}}{m} = 22\left(\frac{\sigma}{\rho_G f_i u_G^2 m}\right)^{0.5}\left(\frac{\rho_G}{\rho_L}\right)^{0.83} \exp\left(0.6\frac{G_{LE}}{\rho_L u_G}\frac{d_t}{d_{32}} + 99 We_{d_t}\right), \tag{14}$$

where We_{d_t} is a Weber number based on the tube diameter and f_i is the interfacial friction factor. Use of this correlation requires knowledge of the mean liquid film thickness, m. For vertical annular flow, the film is distributed symmetrically around the circumference of the pipe, and the film thickness has been related to the Reynolds number of the liquid film (Henstock and Hanratty, 1976). Williams (1990) measured the film thickness for annular flow in the same pipe used in this study and found that it is distributed very asymmetrically, due to the effects of gravity. Below a mean gas velocity of 47 m/s, the film at the top of the pipe was typically of an order of magnitude thinner than the film at the bottom. Use of a mean film thickness, therefore, might not be a good representation of the flow conditions for horizontal flow.

3. Experiments

3.1. Flow loop

The drop size measurements were performed in a flow loop, designed by Williams (1990), which contained a clear acrylic pipe with a diameter of 0.0953 m and a length of 27 m. The pipe was made in sections, and the inside diameter of the pipe at the ends of the sections was machined to ensure smooth transitions. The gas and liquid phases were individually metered and then combined at the inlet by using a simple tee. To ensure that the annular flow was fully developed, drop size measurements were obtained at a distance of 21 m from the inlet, that is, a L/D ratio of 216. A complete description of the flow loop can be found in Williams (1990).

3.2. Drop size measurements

A schematic of the operation of the Malvern Spraytec RTS5008 analyser is shown in Fig. 1. A low power He–Ne laser illuminates the flow field, and particles passing through the beam scatter light. At small forward angles, the scattering is predominantly due to diffraction and the angle of the scattered light is inversely proportional to the size of the drops. The scattered light is detected by a set of concentric annular detectors placed at the focal point of a Fourier lens, which converts the incoming rays of scattered light into a far-field diffraction pattern. Thus, the detector picks up light scattered at a specific angle independent of the position of the drops. Normally, a drop size distribution can be calculated from the energy distribution, but there are mathematical complications with this approach. Instead, a distribution is assumed and this is used to calculate an energy distribution. The values of the parameters describing the size distribution are adjusted until a best fit between the measured and calculated energy is achieved. A 15 parameter (model independent) algorithm is applied to achieve this. The instrument software also includes the patented correction for the effect of multiple scattering, which allows measurements to be made with only a 5% transmission of the incident laser beam. Previously, measurements were only possible

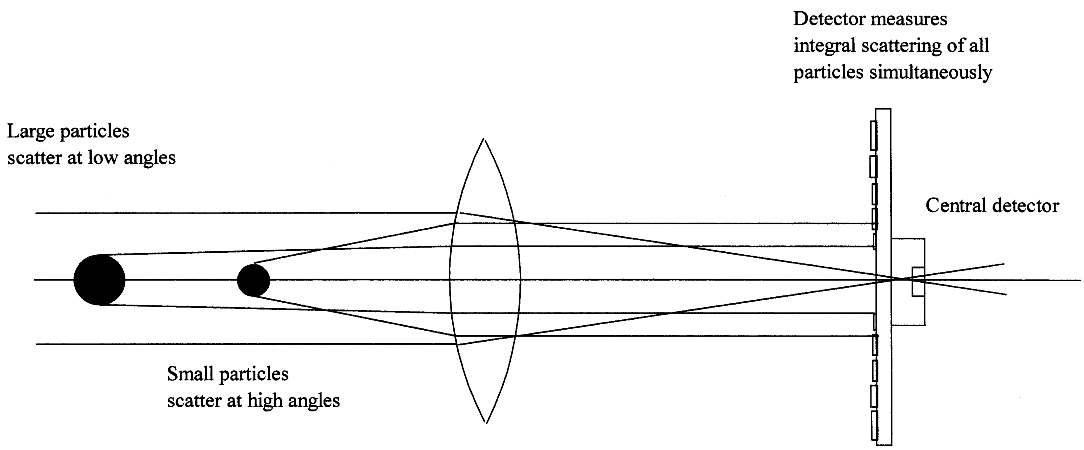

Fig. 1. Schematic of laser diffraction measurement technique.

for transmissions above 60%. Measurements have been made at transmissions down to 20% in the current study. The instrument was equipped with a 450-mm lens which gives a particle size measurement range from 2.25–850 μm.

The drop size measurements were performed in situ, so it was necessary to remove the liquid film from the wall of the pipe to allow the laser beam to pass through the gas core. This was done by using a specially designed test section, shown in Fig. 2, similar to those used by Hay et al. (1996) and by Azzopardi et al. (1996). The flow passes through a porous section and the liquid film, which travels at a lower velocity than the gas and the droplets, is pushed out through the porous section by the pressure in the pipe. The droplets travel at a velocity close to that of the gas, so their large inertias preclude their being removed from the flow. The porous section was placed as close to the measurement point as possible, to minimise the reformation of the film by deposition. The film take-off rate was controlled by a ball valve downstream of the outlet from the porous section. Any remaining film was detoured around the openings used for the laser beam by diverters, made from lengths of o-ring rubber, which were attached to the inside of the pipe.

The laser beam from the Malvern instrument was passed through glass windows, which covered slots cut in the side of the test section to allow access to the flow field. Contamination of the windows by incoming droplets was minimised by placing them some distance away from the flow and by minimising the size of the openings in the side of test section. This was done using very thin acetate sheet with holes that allow the laser beam to pass through. This sheet was rolled into a cylinder and placed inside the test section; the holes in the sheet were aligned with the slots in the section. Several sheets were made with openings at different heights, to allow measurements at

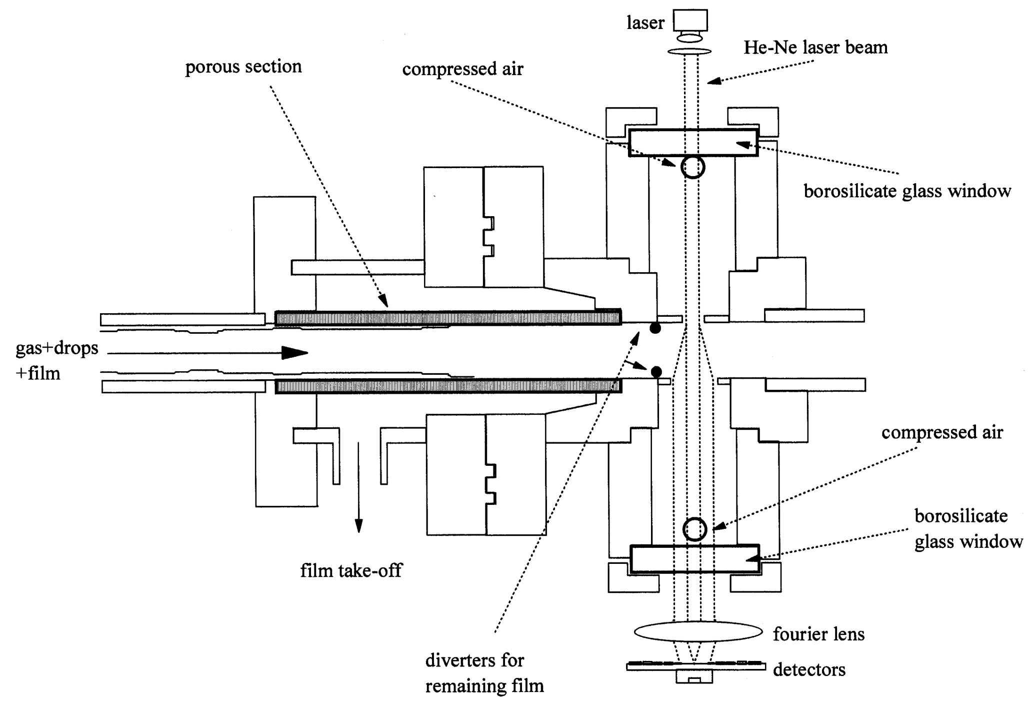

Fig. 2. Diagram of test section employed for the drop size measurements.

different positions. Measurements were obtained at the pipe centre line, and 19 mm above and below it. Measurements could not be made any higher or lower since some of the scattered light could then hit the walls of the pipe. An air purge system was installed to blow air over the internal surfaces of the windows constantly, so as to keep them free of droplets and to maintain a slight positive pressure in the window sections that reduced the number of entering drops.

To change the measurement position, a mechanism, shown in Fig. 3, was constructed to allow the Malvern instrument to perform a vertical traverse over the pipe diameter. The instrument was mounted onto a movable bracket, which was attached to an external frame using four stainless steel rods and a threaded bolt. Rotation of the handle at the top of the mechanism caused the movable bracket to slide up and down on the steel rods. To prevent any alignment problems between the Malvern transmitting and receiving sections, the frame and moveable bracket were rigidly constructed from aluminium. The vertical position of the bracket relative to the external frame was measured by callipers bolted between the bracket and the frame.

Several preliminary studies were made to ensure that there was no influence of the film take-off rate and the air purge upon the drop size distributions. It was discovered that the diverters were sufficient, at low liquid flow rates, to prevent intrusion of the film into the laser beam, without any removal of the liquid film. An experiment was performed at $U_{SG} = 36$ m/s and $U_{SL} = 0.016$ m/s, where the droplet size distribution was measured with the film take-off rate set at zero and at the maximum value obtained with the valve fully open. No differences in the drop size distributions

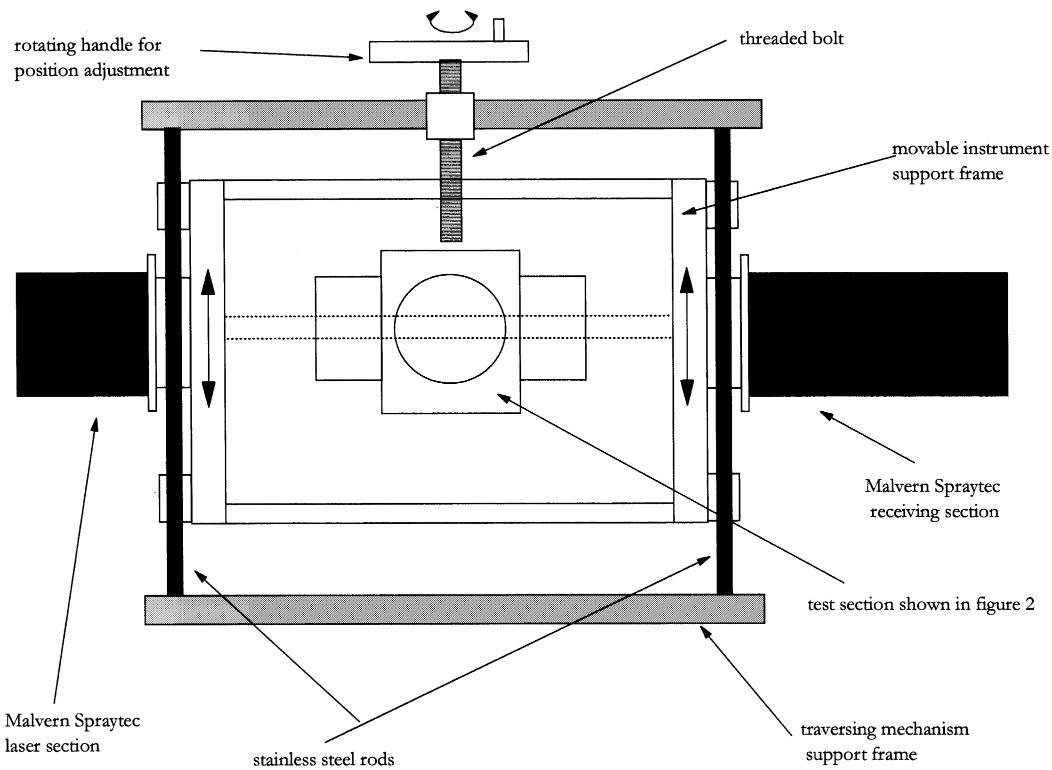

Fig. 3. End-on diagram of the traversing mechanism (some structural details omitted to improve clarity).

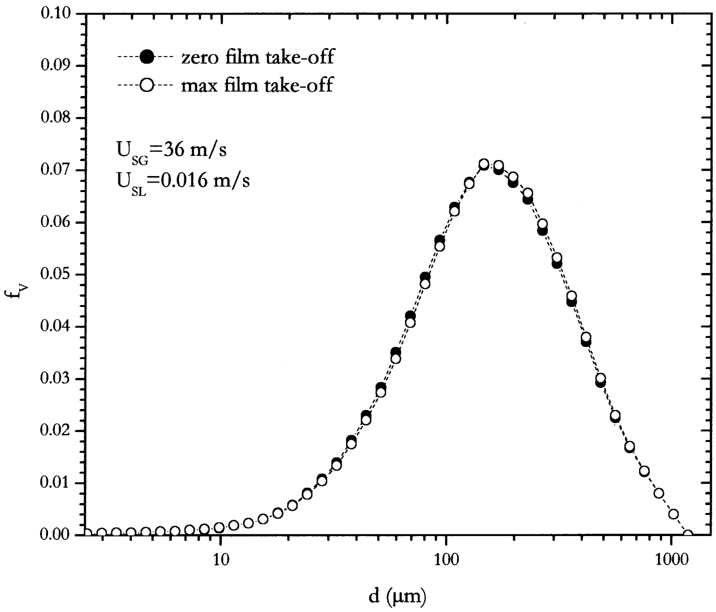

Fig. 4. Effect of film take-off on measured drop size distribution.

were observed; this is illustrated in Fig. 4. In all subsequent runs, the film take-off rate was set to be sufficient to ensure that liquid films did not interfere with the drop size measurements. Similar studies were performed on the influence of the flow of the air purge. No effect was observed if the flow rate was sufficient to prevent contamination of the windows. These results are consistent with the findings of Teixeira (1988).

The distributions obtained from the Malvern instrument were averaged over a sample time of at least 120 s, which gives sample sizes of billions of drops. At the lowest drop concentration used in this study, the entrained liquid mass flux was approximately equal to 3 kg/m^{2}s (Table 1). Assuming a Sauter Mean diameter of 80 μm, this corresponds to a flow of 80,000,000 drops per second.

4. Results

The values of d_{32} obtained at the three measurement positions are shown for four different superficial gas velocities in Figs. 5–8. The measurements made at the centre line were repeated to check for consistency. Significant stratification of the drops is observed at the lowest measured superficial gas velocities. This decreases as the gas velocity increases, and there is only a very small effect of stratification between the bottom and centre at superficial gas velocities of 43 and 50 m/s. The effect of liquid flow rate upon drop diameter is approximately the same at each position. The most significant stratification occurs between the top and the centre of the pipe. This could result from gravitational settling of the droplets and the asymmetry of the liquid film. Larger droplets have a greater terminal velocity, so they settle out of the gas core faster than smaller drops. The

Table 1
Drop size distribution parameters at centre line

Experimental parameters									Upper-limit log-normal parameters					
U_{SG} (m/s)	$\dot{m}_L$ (kg/m^{2}s)	E (Williams, 1990)	G_{LE} (kg/m^{2}s)	Trans. (%)	d_{32} (μm)	d_{v10} (μm)	d_{v50} (μm)	d_{v90} (μm)	d_{v50}	δ	d_{max} (μm)	d_{32} (μm)	a	d_{max}/d_{v50}
30	15.85	0.14	3.08	88.69	113.7	58.2	189.7	560.4	190.0	0.67	1400	115.6	6.4	7.4
30	22.88	0.14	4.34	85.87	111.3	57.7	185.4	534.5	188.0	0.69	1400	117.3	6.4	7.4
30	32.55	0.14	5.74	82.25	111.5	58.0	183.6	516.3	188.0	0.69	1350	117.9	6.2	7.2
30	41.20	0.14	7.00	80.29	112.0	58.4	183.8	510.8	188.0	0.69	1350	117.9	6.2	7.2
30	53.76	0.14	8.96	75.99	113.6	59.5	185.1	504.7	187.0	0.71	1350	120.4	6.2	7.2
30	61.54	0.14	10.08	73.39	114.5	60.3	186.6	503.6	187.0	0.71	1350	120.4	6.2	7.2
30	90.00	0.14	14.00	58.85	124.5	66.4	204.7	528.0	205.0	0.73	1350	136.0	5.6	6.6
30	122.00	0.14	18.90	48.89	134.0	71.5	221.9	557.1	222.0	0.72	1350	146.3	5.1	6.1
36	15.85	0.26	5.72	88.97	88.7	47.5	149.6	426.0	150.2	0.73	1500	97.9	9.0	10.0
36	22.88	0.255	7.91	77.53	90.0	48.6	151.4	419.9	151.5	0.75	1500	100.2	8.9	9.9
36	32.55	0.25	10.25	71.31	93.4	51.0	157.7	427.2	157.5	0.75	1500	105.3	8.5	9.5
36	41.20	0.24	12.00	67.52	96.9	53.1	164.1	438.2	163.9	0.75	1500	109.8	8.2	9.2
36	53.76	0.23	14.72	59.63	105.3	57.5	179.1	472.2	178.5	0.75	1450	119.6	7.1	8.1
36	61.54	0.22	15.84	56.92	108.9	59.4	184.6	482.6	184.1	0.76	1450	125.0	6.9	7.9
43	15.85	0.440	9.68	66.81	76.0	41.7	128.5	329.3	126.7	0.80	1500	88.2	10.8	11.8
43	22.88	0.435	13.49	59.52	79.0	43.3	133.6	333.4	133.6	0.82	1500	94.7	10.2	11.2
43	32.55	0.430	17.63	51.41	85.7	46.9	145.6	366.9	143.2	0.82	1500	101.8	9.5	10.5
43	41.20	0.420	21.00	45.17	91.4	50.1	157.1	397.2	157.1	0.82	1500	112.0	8.5	9.5
43	53.76	0.410	26.24	36.94	99.4	54.4	172.8	436.2	170.5	0.80	1500	119.8	7.8	8.8
43	61.54	0.400	28.80	33.76	102.9	56.3	178.9	452.3	180.6	0.79	1500	125.8	7.3	8.3
50	15.85	0.560	12.32	57.14	60.2	35.3	106.7	279.0	106.0	0.83	1700	75.2	15.0	16.0
50	22.88	0.540	16.74	46.73	65.2	37.9	114.3	288.1	117.0	0.85	1550	84.6	15.2	13.2
50	32.55	0.530	21.73	37.08	72.6	41.5	126.9	318.3	127.0	0.84	1550	91.3	11.2	12.2
50	41.20	0.520	26.00	31.3	79.0	44.7	138.8	352.0	139.0	0.82	1600	98.5	10.5	11.5
50	53.76	0.510	32.64	24.79	86.8	48.6	153.1	388.5	150.9	0.78	1400	103.5	8.3	9.3
50	61.54	0.500	36.00	21.61	92.5	51.5	163.0	415.0	163.0	0.78	1550	112.0	8.5	9.5

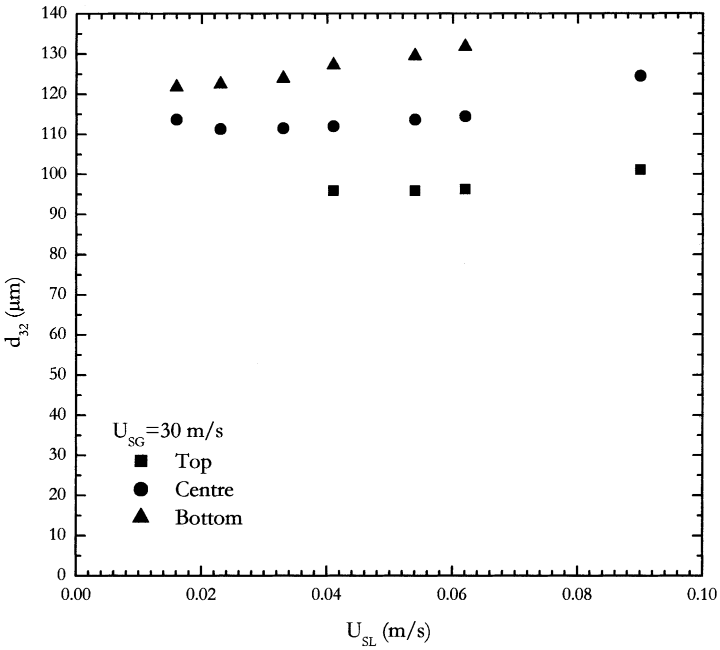

Fig. 5. Effect of measurement position on d_{32} at $U_{SG} = 30$ m/s.

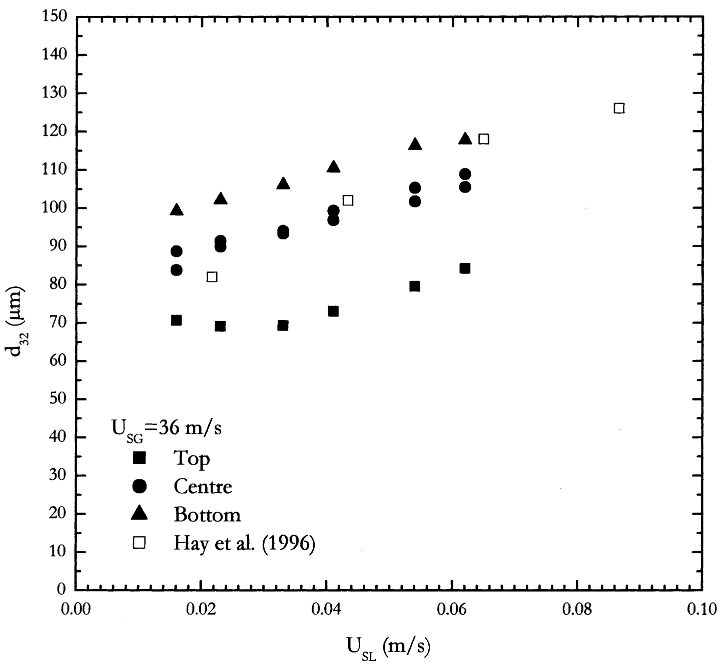

Fig. 6. Effect of measurement position on d_{32} at $U_{SG} = 36$ m/s.

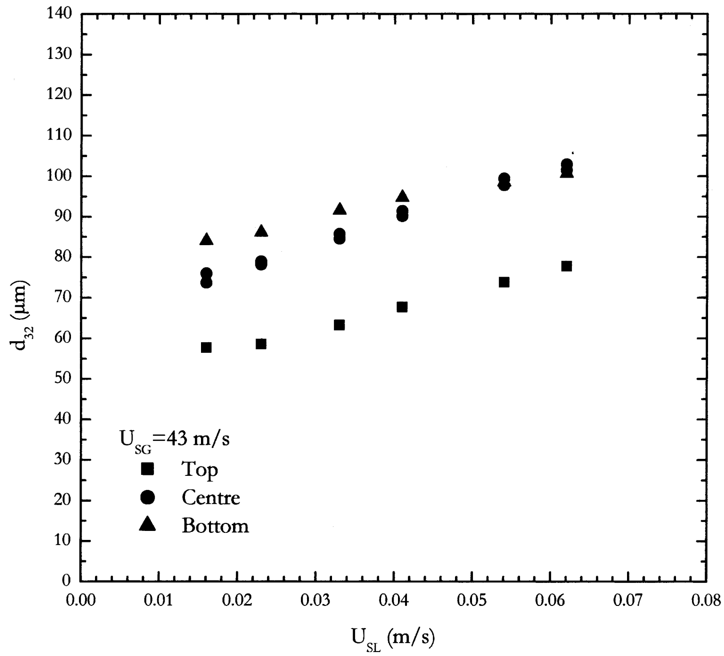

Fig. 7. Effect of measurement position on d_{32} at $U_{SG} = 43$ m/s.

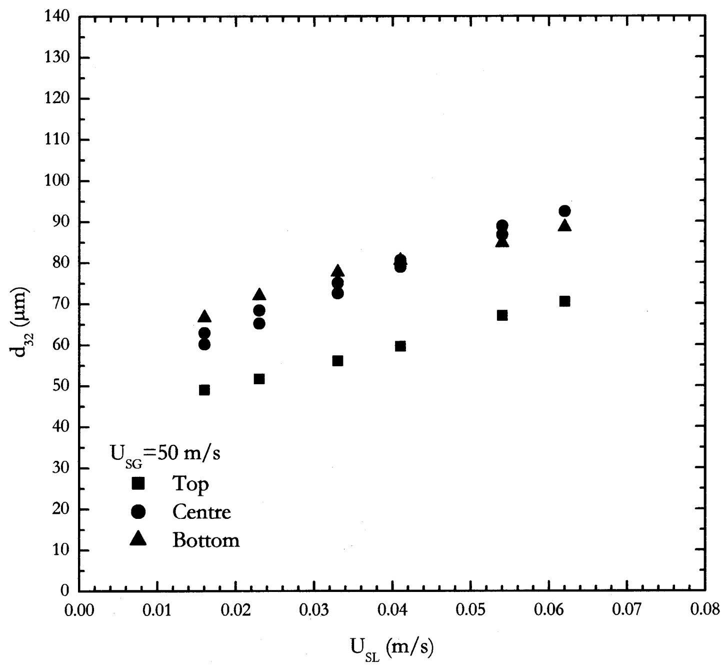

Fig. 8. Effect of measurement position on d_{32} at $U_{SG} = 50$ m/s.

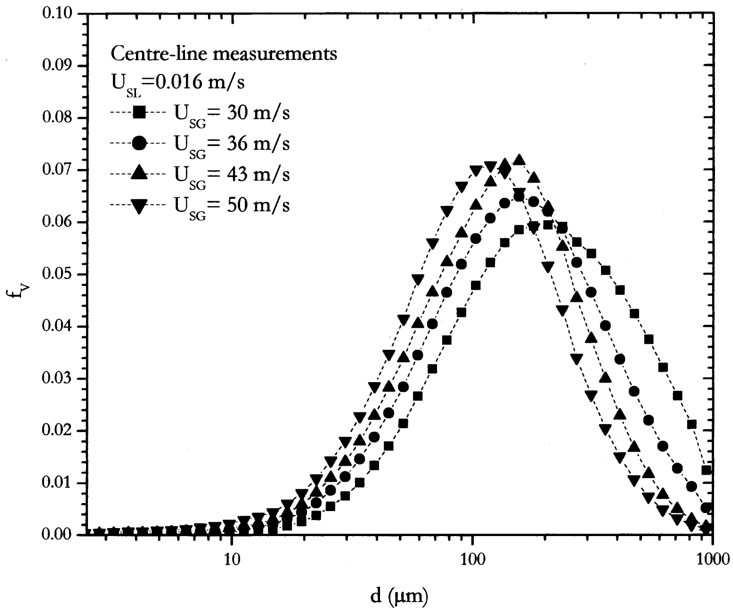

Fig. 9. Sample volume distributions obtained at the centre line at $U_{SL} = 0.016$ m/s.

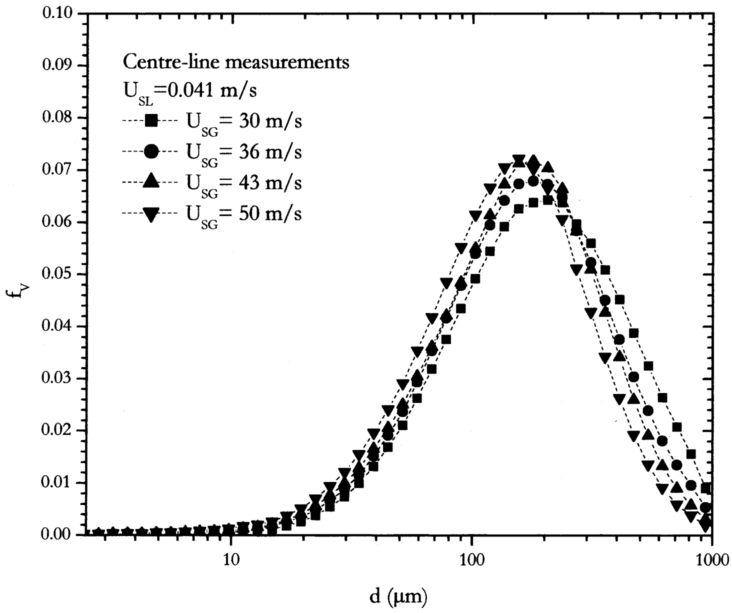

Fig. 10. Sample volume distributions obtained at the centre line at $U_{SL} = 0.041$ m/s.

larger drops are, therefore, concentrated towards the bottom half of the pipe. Due to the asymmetry of the liquid film, it is reasonable to assume that droplets forming from waves on the bottom of the pipe will be bigger than those that form closer to the top. The data in Fig. 6, obtained at a U_{SG} of 36 m/s, are compared to the data of Hay et al. (1996), obtained for vertical upflow in a 0.042-m pipe. There is some agreement at the bottom and centre positions; however, the data of Hay et al. (1996) show a stronger influence of liquid flow rate.

Drop size distributions, shown in Figs. 9 and 10, are unimodal; there is a clear increase in the importance of small drops as the gas flow rate is increased. This shift is less pronounced at higher U_{SL}, as would be expected from the measurements of d_{32} already presented. At the lowest gas flow rate, the distribution tail is not well defined. This is expected since the Malvern instrument has an upper limit in the sizes that it can measure accurately. This could be overcome by using a lens with a longer focal length, which unfortunately is not an option for this system. Various parameters characterizing the drop size distributions are summarised in Tables 1–3.

5. Discussion

Azzopardi (1985), Fore and Duker (1995) and Hay et al. (1996) suggested that the mean drop size for vertical annular flows should depend linearly on the entrained liquid mass flux, or drop concentration. The entrained liquid mass flux was obtained from the data of Williams (1990), who sampled the droplet flux isokinetically in the same flow loop over the same ranges of flow conditions. Indirect determination of the entrainment from the flow rate of liquid exiting the film take-off unit was not attempted due to the difficulty of removing the entire film. The centre-line data are plotted against a dimensionless liquid concentration, $G_{LE}/(\rho_L U_G)$, in Fig. 11 and a linear dependency is seen at high gas velocities. However, the data taken at the superficial gas velocities of 30 and 36 m/s appear to pass through a minimum; i.e. d_{32} decreases with liquid flow rate at low liquid flow rates. This effect was also observed by Azzopardi (1985), who attributed this behaviour to changes in the atomisation mechanisms suggested by visualisation experiments (Azzopardi et al., 1983). It is possible that this effect may occur at higher superficial gas velocities and lower liquid flow rates, but the droplet concentration was insufficient to obtain reliable measurements below a liquid superficial velocity of 0.016 m/s. Over the range of liquid concentrations studied, the measured d_{32} are approximated by

$$d_{32}U_G^{1.1} = 4.848\frac{G_{LE}}{\rho_L U_G} + 0.0038 \tag{15}$$

as shown by the lines in Fig. 11. Good agreement is noted, except for the lowest gas velocity of 30 m/s. This equation can be made non-dimensional by using a length scale, λ_A or d_t as follows:

$$\left(\frac{d_{32}U_G^2\rho_G}{\sigma}\right)^{0.55}\left(\frac{d_{32}}{\lambda_A}\right)^{0.45} = 332.9\frac{G_{LE}}{\rho_L U_G} + 0.261, \tag{16a}$$

$$\left(\frac{d_{32}U_G^2\rho_G}{\sigma}\right)^{0.55}\left(\frac{d_{32}}{d_t}\right)^{0.45} = 66.5\frac{G_{LE}}{\rho_L U_G} + 0.052. \tag{16b}$$

These are a modification of Eq. (10) suggested by Tatterson et al. (1977).

Table 2
Drop size distribution parameters at 3/4″ above centre line

Experimental parameters									Upper-limit log-normal parameters					
U_{SG} (m/s)	$\dot{m}_L$ (kg/m^{2}s)	E (Williams, 1990)	G_{LE} (kg/m^{2}s)	Trans. (%)	d_{32} (μm)	d_{v10} (μm)	d_{v50} (μm)	d_{v90} (μm)	d_{v50}	δ	d_{max} (μm)	d_{32} (μm)	a	d_{max}/d_{v50}
30	41.20	0.14	7.0	86.05	95.9	48.3	162.4	488.0	164.0	0.69	1400	101.3	7.5	8.5
30	53.76	0.14	8.96	83.23	95.9	48.9	163.2	476.3	164.7	0.69	1350	102.2	7.2	8.2
30	61.54	0.14	10.08	81.31	96.3	49.2	163.9	472.4	165.1	0.69	1350	103.2	7.2	8.2
30	90.00	0.14	14.00	71.03	101.1	52.4	173.4	465.7	172.6	0.72	1350	111.4	6.8	7.8
30	122.00	0.14	18.90	63.68	106.3	55.3	183.2	473.4	181.1	0.72	1350	118.3	6.5	7.5
36	15.85	0.26	5.72	86.24	71.2	37.9	122.5	366.7	123.6	0.70	1200	77.6	8.7	9.7
36	22.88	0.255	7.91	81.95	69.6	37.3	120.2	342.5	120.0	0.73	1300	77.5	9.8	10.8
36	32.55	0.25	10.25	77.47	69.7	37.7	121.7	328.9	120.0	0.74	1350	78.6	10.3	11.3
36	41.20	0.24	12.00	72.16	73.5	39.4	130.2	349.0	128.0	0.74	1350	84.0	9.5	10.5
36	53.76	0.23	14.72	65.23	80.1	42.4	145.0	378.6	141.8	0.73	1400	92.3	8.9	9.9
36	61.54	0.22	15.84	59.84	84.8	44.6	156.4	406.5	152.4	0.72	1400	98.3	8.2	9.2
36	90.00	0.200	20.00	48.35	100.0	52.2	189.4	473.8	184.1	0.71	1400	118.1	6.6	7.6
36	122.00	0.200	27.00	41.14	109.3	56.5	208.9	506.3	202.8	0.71	1300	131.5	5.4	6.4
43	15.85	0.440	9.68	76.28	57.9	32.2	104.4	308.7	104.4	0.73	1500	66.7	13.4	14.4
43	22.88	0.435	13.49	70.74	59.0	32.7	106.0	294.6	104.9	0.75	1400	69.1	12.3	13.3
43	32.55	0.430	17.63	63.1	63.5	34.8	117.4	317.9	114.9	0.74	1400	75.0	11.2	12.2
43	41.20	0.420	21.00	57.08	68.0	36.8	129.4	345.0	125.9	0.72	1350	8.7	9.7	10.7
43	53.76	0.410	26.24	49.07	74.1	39.5	145.4	379.2	145.0	0.73	1300	94.7	8.0	9.0
43	61.54	0.400	28.80	44.53	78.2	41.3	156.7	404.6	150.8	0.69	1300	93.7	7.6	8.6
43	90.00	0.400	40.00	33.07	99.0	51.5	206.0	504.2	199.5	0.65	1150	119.1	4.8	5.8
43	122.00	0.400	54.00	29.63	109.3	56.3	230.9	557.5	223.6	0.64	1150	133.3	4.1	5.1
50	15.85	0.560	12.32	67.48	49.2	228.3	93.4	293.1	94.0	0.71	1400	59.2	13.9	14.9
50	22.88	0.540	16.74	58.51	51.9	29.6	99.5	295.5	98.9	0.72	1450	63.1	13.7	14.7
50	32.55	0.530	21.73	49.36	56.5	31.6	111.2	308.9	108.5	0.72	1450	69.3	12.4	13.4
50	41.20	0.520	26.00	42.76	59.9	33.2	121.8	326.1	117.1	0.71	1350	74.2	10.5	11.5
50	53.76	0.510	32.64	33.89	67.7	36.4	143.9	372.4	137.8	0.68	1300	84.1	8.4	9.4
50	61.54	0.500	36.00	30.53	71.1	37.9	156.8	396.7	149.4	0.66	1200	89.2	7.0	8.0

Table 3
Drop size distribution parameters at 3/4″ below centre line

Experimental parameters									Upper-limit log-normal parameters					
U_{SG} (m/s)	$\dot{m}_L$ (kg/m^{2}s)	E (Williams, 1990)	G_{LE} (kg/m^{2}s)	Trans. (%)	d_{32} (μm)	d_{v10} (μm)	d_{v50} (μm)	d_{v90} (μm)	d_{v50}	δ	d_{max} (μm)	d_{32} (μm)	a	d_{max}/d_{v50}
30	15.85	0.14	3.08	82.64	121.8	61.1	208.5	587.7	211.4	0.65	1300	125.9	5.1	6.1
30	22.88	0.14	4.34	79.06	122.5	61.8	209.0	573.8	210.8	0.66	1300	127.8	5.2	6.2
30	32.55	0.14	5.74	75.53	123.9	62.8	211.5	570.4	212.8	0.67	1300	130.4	5.1	6.1
30	41.20	0.14	7.00	71.44	127.2	64.8	218.9	577.7	219.6	0.67	1300	135.1	4.9	5.9
30	53.76	0.14	8.96	67.45	129.5	66.1	223.9	584.6	224.0	0.67	1300	138.0	4.8	5.8
30	61.54	0.14	10.08	64.55	131.8	67.4	229.4	597.1	229.3	0.66	1300	140.8	4.7	5.7
36	15.85	0.26	5.72	70.29	99.3	51.6	170.7	466.4	170.7	0.70	1300	108.4	6.6	7.6
36	22.88	0.255	7.91	65.48	102.2	53.3	176.8	475.1	176.2	0.70	1300	112.2	6.4	7.4
36	32.55	0.25	10.25	60.7	106.1	55.3	186.3	496.1	185.6	0.69	1300	116.9	6.0	7.0
36	41.20	0.24	12.00	55.5	110.5	57.3	195.1	515.5	193.8	0.69	1300	121.4	5.7	6.7
36	53.76	0.23	14.72	48.71	116.4	60.1	208.7	548.6	207.2	0.67	1300	127.8	5.3	6.3
36	61.54	0.22	15.84	46.42	117.8	60.8	211.7	552.5	210.0	0.67	1300	129.5	5.2	6.2
43	15.85	0.44	9.68	60.11	84.1	45.3	148.8	413.2	148.5	0.72	1300	95.4	7.8	8.8
43	22.88	0.435	13.49	53.89	86.2	46.4	153.7	414.7	152.6	0.72	1300	98.6	7.5	8.5
43	32.55	0.43	17.63	46.68	91.6	48.8	164.5	435.5	163.2	0.71	1300	104.5	7.0	8.0
43	41.20	0.42	21.00	41.74	94.8	50.5	172.7	461.3	171.3	0.70	1300	108.1	6.6	7.6
43	53.76	0.41	26.24	35.73	98.6	52.2	179.8	478.7	178.3	0.69	1300	111.8	6.3	7.3
43	61.54	0.4	28.80	31.93	100.7	53.1	184.1	486.4	182.5	0.69	1300	113.9	6.1	7.1
50	15.85	0.56	12.32	49.63	66.7	37.7	124.1	358.1	123.0	0.75	1300	80.9	13.6	14.6
50	22.88	0.54	16.74	41.49	72.0	40.5	134.4	390.5	133.5	0.74	1800	86.7	12.5	13.5
50	32.55	0.53	21.73	33.32	77.7	43.4	146.5	419.6	145.4	0.73	1800	93.7	11.4	12.4
50	41.20	0.52	26.00	29.54	80.5	44.7	153.1	434.3	151.6	0.72	1800	96.9	10.9	11.9
50	53.76	0.51	32.64	23.72	84.8	46.6	162.0	455.1	161.0	0.70	1500	100.6	8.3	9.3
50	61.54	0.5	36.00	20.48	88.6	48.3	170.8	476.9	169.3	0.69	1500	104.6	7.9	8.9

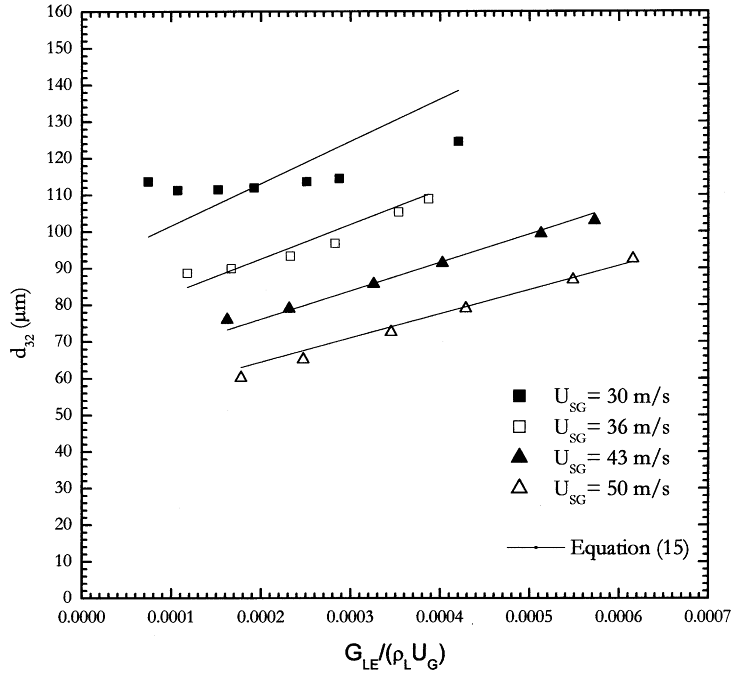

Fig. 11. Development of correlation for d_{32} at centre line.

Fig. 12 shows that the effects of liquid flux are consistently underpredicted by the modified correlation developed by Azzopardi (1985, Eq. 12). This equation was developed from data obtained for vertical upflow in pipes with smaller diameters, so a comparison could be considered as unreasonable. However, Hay et al. (1996) and Fore and Duker (1995) also observed similar discrepancies from the Azzopardi (1985) equation in their studies of vertical annular flow. The differences may be partly explained as due to effects of multiple scattering. The correction for this effect employed by the Malvern Spraytec instrument is presented for the centre-line data in Figs. 13 and 14. It is greatest at the highest gas and liquid flow rates. This is to be expected because Williams (1990) showed that drop concentrations in the 0.0953-m pipe are strong functions of gas velocity. The uncorrected values of d_{32} are lower and are less sensitive to changes in liquid flow rate. The laser diffraction instrument used by Azzopardi (1985), was an earlier version which did not have a feature to correct for the multiple scattering.

The constants in the modified Azzopardi equation, A and B, have been re-evaluated for the current data and the data of Hay et al. (1996). The results are shown in Table 4. The equation predicts the centre-line values of d_{32} to within 10%. If the centre-line data is reprocessed without the multiple scattering correction, the values of the constants become much closer to the values given by Pan and Hanratty (2000). The values of the constants for the data of Hay et al. (1996) are close to those obtained from the current study.

The comparison of the data of Hay, for $d_t = 0.042$ m, with the data obtained in this investigation, $d_t = 0.0953$ m, in Fig. 6, would suggest only a small effect of pipe diameter, so that Eq. (16a) could be appropriate. Eq. (16b) predicts that drop sizes in a 0.0953-m pipe should be 45% higher than in a 0.042-m pipe). However, since Hay's measurements were in a vertical pipe, one

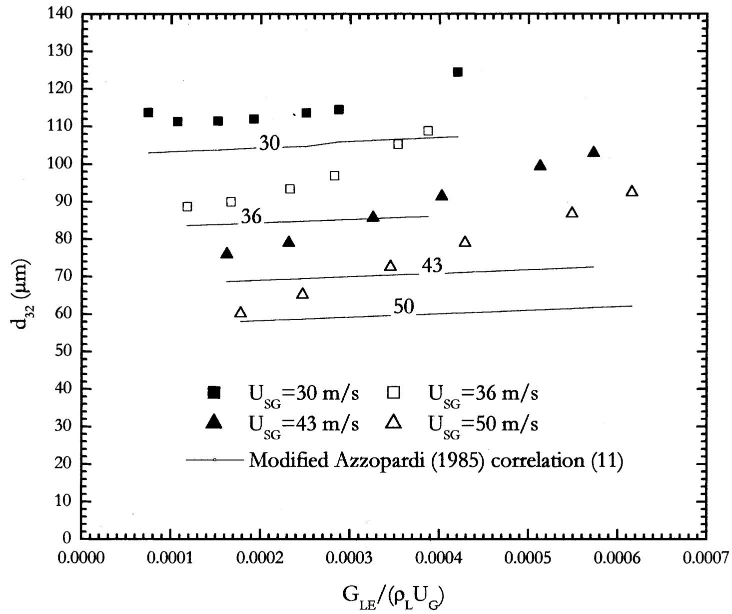

Fig. 12. Comparison of centre-line data with the correlation of Azzopardi (1985).

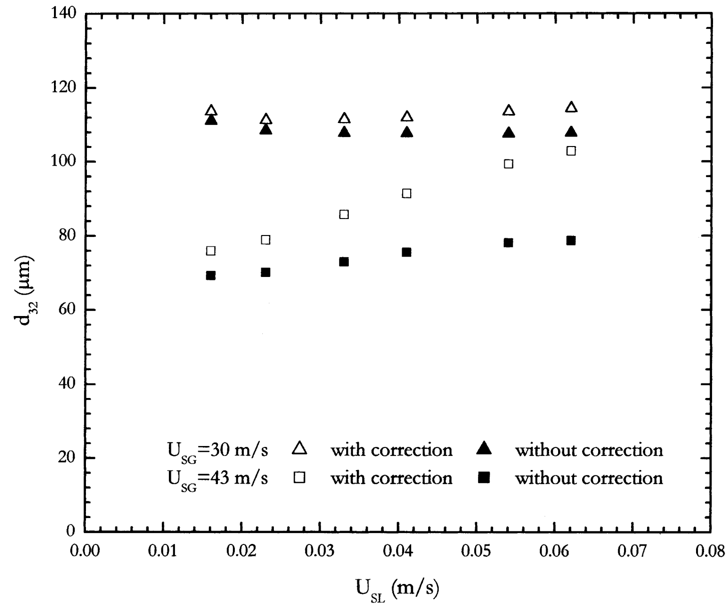

Fig. 13. Effect on d_{32} of the multiple scattering correction.

cannot conclude, definitely, that there is a very small effect of pipe diameter. Clearly data are needed for several pipe diameters. These should be obtained with the same measurement technique.

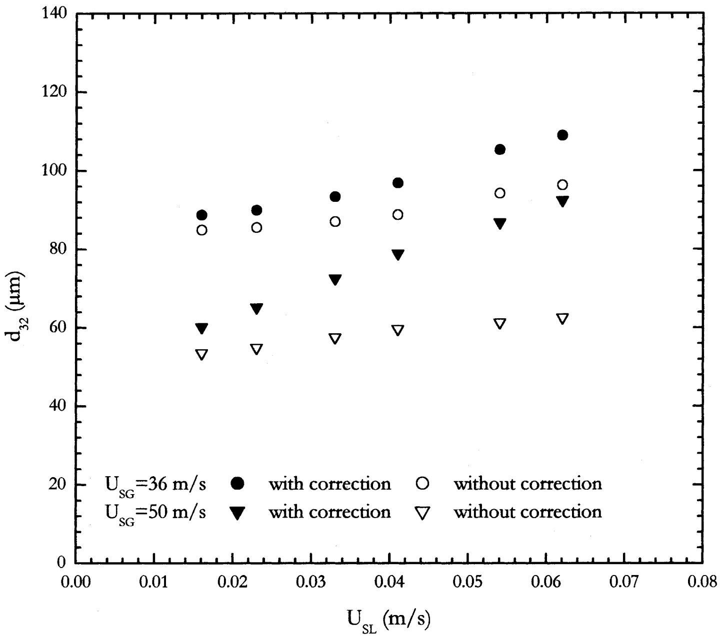

Fig. 14. Effect on d_{32} of the multiple scattering correction.

Table 4
Constants in modified equation of Azzopardi (1985)

Data set	*A*	*B*
Pan and Hanratty (2000)	0.33	3.5
Centre-line data (multiple scattering correction)	0.33	18.6
Centre-line data (no correction)	0.34	4.2
Top data	0.25	17.0
Bottom data	0.38	14.7
Hay et al. (1996)	0.29	15.8

The measurements are compared with different distribution functions in Fig. 15. The Rosin–Rammler equation overpredicts the volume contribution of small drops and underpredicts the volume contribution of large drops; it is, therefore, unsuitable. The upper-limit log-normal and log-normal distributions are much better. However, both underpredict the volume contribution of small drops. The upper-limit log-normal function provides a slightly better fit to the volume contributions of large drops. A log–probability plot shows that a good fit is obtained between the data and the upper limit log-normal distribution function over most of the size range (Fig. 16). Values of d_{32} obtained from this distribution function are typically 10–15 μm higher than the experimental values; this is due to the underprediction of the number of small drops. The values of d_{32} obtained from the raw data are therefore more reliable. The distribution parameters used to calculate the distribution functions are given in Tables 1–3.

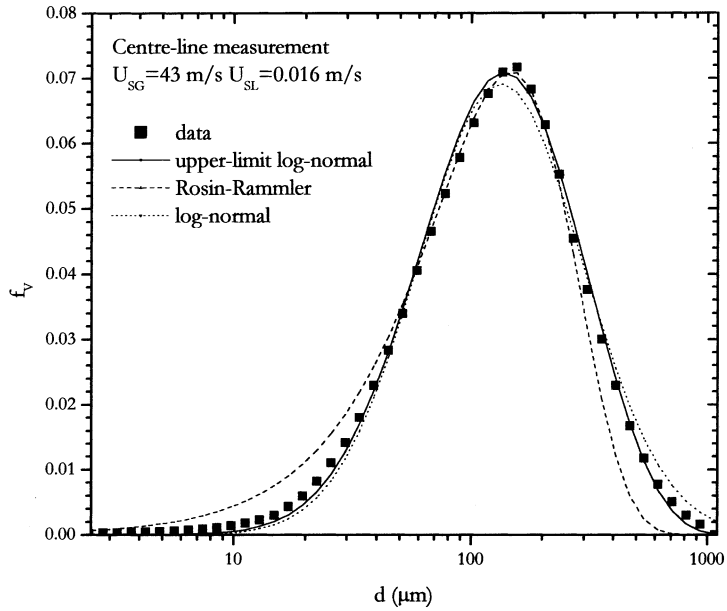

Fig. 15. Example of distribution function fitting to the experimental data.

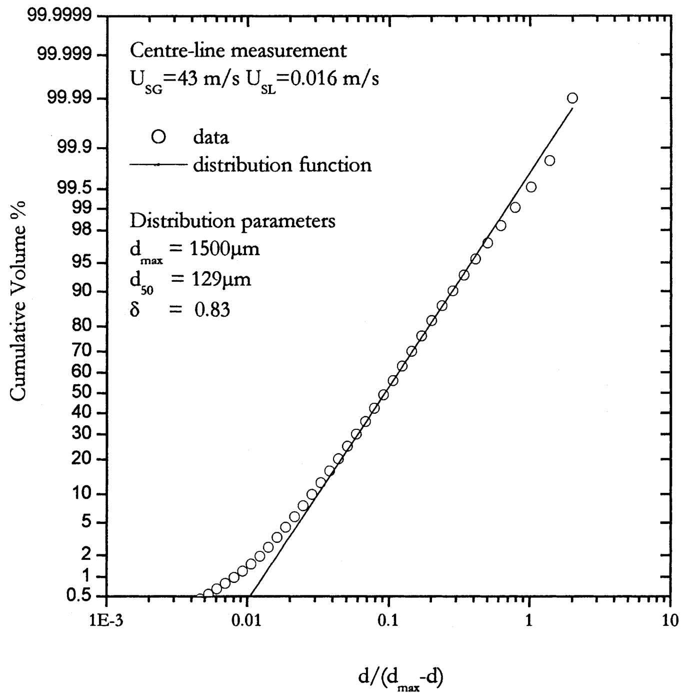

Fig. 16. Log–probability plot for upper limit log-normal distribution fit for the data in Fig. 15.

Fore and Duker (1995) suggested that the use of unimodal distribution functions could be questionable, since their measurements of drop size distributions were bimodal. The reasons for this are not clear, but a possible explanation could be that the measurement range was too narrow. The lower size limit for their technique was 10 μm; a significant amount of drops detected in this work were below this size. Another possible reason could be that their measurements were taken locally at the centre of the pipe; the measurements in this study are an ensemble average over a horizontal chord through the whole width of the pipe. No bimodal distributions were observed in this study, with effective sample sizes of billions of drops.

The determination of the parameters for the upper limit log-normal function requires knowledge of the largest droplet size present in the distribution, d_{max}. The volume distributions obtained from the Malvern particle sizer are calculated from the intensity of the scattered light, and are presented as a histogram of 60 logarithmic size bands. The number of droplets detected in each size band is not calculated. Therefore, d_{max} cannot be determined directly. It is possible to determine d_{max} directly from techniques which physically count the number of drops, such as the photographic technique employed by Hay et al. (1996), but the accuracy is dependent upon the sample size, i.e. on the number of droplets measured. Azzopardi and Hibberd (1994) studied data from various workers and showed that d_{max} increases with sample size. The values of d_{max} determined in the current work were chosen to give the best straight line on a log–probability plot, at large drop sizes. The distribution function, however, was found to be insensitive to small changes in d_{max}, so the values obtained are approximate.

A consequence of the use of a measurement technique which can detect very small droplets is the determination of higher ratios of d_{max}/d_{v50} than has been obtained from other workers. Tatterson et al. (1977) and Wicks and Dukler (1966) suggested that d_{max}/d_{v50} should be a weak function of flow variables and obtained a value of approximately 3–5. Ratios ranging from 7–11 were obtained in the current work, as shown in Tables 1–3.

6. Concluding remarks

Measurements of drop size distributions in horizontal annular flow have shown stratification of drop size and a dependence of $d_{32} \sim U_G^{-1.1}$. The results agree with results obtained for vertical annular flow. The data show stronger effects of liquid flow rate, closer to that shown by Hay et al. (1996), than observed by Azzopardi (1985). This may be due to improvements in the measurement technique. The drop size distributions are best represented by an upper limit log-normal distribution function, but there is consistent underprediction of the number of small drops.

Acknowledgements

This work was supported by the Energy Research Program of the Office of Basic Energy Sciences at the Department of Energy under Grant DOE DEF G02-86ER-13556. The invaluable advice of Prof. Barry Azzopardi on the execution of the experiments is gratefully acknowledged.

References

Ambrosini, W., Andreussi, P., Azzopardi, B.J., 1991. A physically based correlation for drop size in annular flow. Int. J. Multiphase Flow 17, 497–507.

Andreussi, P, Romano, G., Zanelli, S., 1978. Drop size distribution in annular mist flow. In: Proceedings of the First Conference on Liquid Atomisation in Spray Systems, Tokyo, August, pp. 27–31.

Azzopardi, B.J., 1985. Drops sizes in annular two-phase flow. Exp. Fluids. 3, 53–59.

Azzopardi, B.J., 1997. Drops in annular two-phase flow. Int. J. Multiphase Flow 23, 1–53.

Azzopardi, B.J,. Hibberd, S., 1994. Determination of maximum drop sizes in annular gas–liquid flow. In: Proceedings of the Sixth International Conference on Liquid Atomisation and Spray Systems, pp. 962 969.

Azzopardi, B.J., Freeman, G., Whalley, P.B., 1978. Drop sizes in annular two-phase flow. ASME Winter Annual Meeting. Published in Topics in Two-phase Flow and Heat Transfer, pp. 165–173.

Azzopardi, B.J., Freeman, G., King, D.J., 1980. Drop sizes and deposition in annular two-phase flow. UKAEA Report, AERE R9634.

Azzopardi, B.J., Piearcey, A., Jepson, D.M., 1991. Drop size measurements for annular twophase flow in a mm diameter vertical tube. Exp. Fluids 11, 191–197.

Azzopardi, B.J., Taylor, S., Gibbons, D.B., 1983. Annular two-phase flow in large diameter pipes. In: Proceedings of the International Conference on Phyical Modelling of Multi-Phase Flow, 9–21 April, Coventry, pp. 256–267.

Azzopardi, B.J., Zaidi, S.H., Sudlow, C.A., 1996. The effect of inclination on drop sizes in annular gas–liquid flow. European Two-Phase Flow group Meeting, Grenoble, 2–5 June.

Combellack, J.H., Matthews, G.A., 1981. Droplet spectra measurements of fan and cone atomisers using a laser diffraction technique. J. Aerosol. Sci. 12, 529–540.

Cousins, L.B., Hewitt, G.F., 1968. Liquid phase mass transfer in annular two-phase flow: droplet deposition and liquid entrainment. UKAEA Report AERE-R5657.

Crowe, C., Sommerfeld, M., Tsuji, Y., 1998. Multiphase Flow with Droplets and Particles. CRC Press, Boca Raton.

Fore, L.B., Dukler, A.E., 1995. The distribution of droplet size and velocity in gas–liquid annular flow. Int. J. Multiphase Flow 21, 137–149.

Gibbons, D.B., 1985. Drop formation in annular two-phase flow. Ph.D. thesis, University of Birmingham.

Harvill, T.L., Holve D.J., Hoog, 1997. US patent 5,619,324. 8th April 1997.

Hay, K.C, Liu, Z.C., Hanratty, T.J., 1996. Relation of deposition rate to drop size when the rate law is non-linear. Int. J. Multiphase Flow 22, 829–848.

Henstock, W.H., Hanratty, T.J., 1976. The interfacial drag and height of the wall layer in annular flows. AIChE J. 22 (6), 990–1000.

Jepson, D.M., 1992. Vertical annular flow: the effect of physical properties. D.Phil. thesis, University of Oxford.

Jepson, D.M., Azzopardi, B.J., Whalley, P.B., 1989. The effects of gas properties on drops in annular flow. Int. J. Multiphase Flow 15, 327–339.

Jepson, D.M., Azzopardi, B.J., Whalley, P.B., 1990. The effect of physical properties on drop size in annular flow. In: Proceedings of the Ninth International Heat Transfer Conference, Jerusalem, vol. 6, pp. 95–100.

Lopes, J.C.B., Dukler, A.E., 1985. Droplet sizes, dynamics and deposition in vertical annular flow. US Nucl. Regulatory Commission, Washington DC, USA, Report NUREG/CR-4424.

McVean, S.S., Wallis, G.B., 1969. Experience with the Wicks–Dukler probe for measuring drop size distribution in sprays. Report, Dartmouth College, Hanover NH.

Mugele, R.A., Evans, H.D., 1951. Droplet size distribution in sprays. Ind. Engrg. Chem. 43, 1915–1931.

Pan, L., Hanratty, T.J., 2000. A correlation of entrainment for annular flow in a horizontal pipe. Int. J. Multiphase Flow?.

Pogson, J.T., Roberts, J.H., Waibler, P.J., 1970. An investigation of the liquid disintegration in annular mist flow. Trans ASME J. Heat Transfer 92, 651–658.

Ribeiro, A.M., Bott, T.R., Jepson, D.M., 1995. Drop size and entrainment measurements in horizontal flow. In: G.P. Celata, R.K. Shah Pub Edizione (Eds.), International Conference on two-phase flow modelling and experimentation. Rome, 9–11 October, ETS, Pisa, vol. II, pp. 665–674.

Rosin, P., Rammler, E., 1933. Laws governing the fineness of powdered coal. J. Inst. Fuel 7, 29–36.

Semiat, R., Dukler, A.E., 1981. Simultaneous measurement of size and velocity of bubbles and drops: a new optical technique. AIChE J. 27, 148–159.

Simmons, M.J.H., Zaidi, S.H., Azzopardi, B.J., 2000. Comparison of laser based drop size measurement techniques and their application to dispersed liquid-liquid pipe flow. Optical Eng. 39 (2), 505–509.

Swithenbank, J., Beer, J.M., Taylor, D.S., Abbot, D., McCreath, G.C., 1976. A laser diagnostic for the measurement of droplet and particle size distributions. Prog. Astronaut. Aeronaut. 1, 421–447.

Tatterson, D.F., Dallman, J.C., Hanratty, T.J., 1977. Drop sizes in annular gas–liquid flows. AIChE .J 23, 68–76.

Teixeira, J.C.F., 1988. Turbulence in annular two phase flow. Ph.D. thesis, University of Birmingham.

Teixeira, J.C.F., Azzopardi, B.J., Bott, T.R., 1988. The effect of inserts on drop size in vertical annular flow. In: Proceedings of the Second UK National Heat Transfer Conference, Strathclyde, vol. Ii, pp. 1281–1296.

Wicks, M., Dukler, A.E., 1966. In-situ measurements of drop size distribution in two-phase flow: a new method for electrically conducting liquids. Third International Heat Transfer Conference, Chicago.

Williams, L.R., 1990. Effect of pipe diameter on horizontal annular two-phase flow. PhD thesis, University of Illinois, Urbana.

Zaidi, S.H., Altunbas, A., Azzopardi, B.J., 1998. A comparative study of phase Doppler and laser diffraction techniques to investigate drop sizes in annular two-phase flow. Chem. Engrg. J. 71, 135–143.